Zoology 156 (2023) 126067

Contents lists available at ScienceDirect

Zoology

journal homepage: www.elsevier.com/locate/zool

A histochemical and morphological study of the mucus producing pedal gland system in *Latia neritoides* (Mollusca; Gastropoda; Hygrophila)

Sophie Greistorfer [a], Janek von Byern [b], Ingrid Miller [c], Victor Benno Meyer-Rochow [d,e], Robert Farkas [f], Gerhard Steiner [a,*]

[a] Unit for Integrative Zoology, Department of Evolutionary Biology, University of Vienna, Austria
[b] Ludwig Boltzmann Institute for Experimental and Clinical Traumatology, Austrian Cluster for Tissue Regeneration, Vienna, Austria
[c] Institute of Medical Biochemistry, University of Veterinary Medicine Vienna, Austria
[d] Department of Ecology and Genetics, Oulu University, Oulu SF-90140, Finland
[e] Agricultural Science and Technology Research Institute, Andong National University, Andong 36729, Republic of Korea
[f] Laboratory of Developmental Genetics, Institute of Experimental Endocrinology, Biomedical Centre, Slovak Academy of Sciences, Bratislava, Slovakia

ARTICLE INFO

Keywords:
Ultrastructural analyses
Limnic
Bioadhesive
Lucent
Defence secretion

ABSTRACT

The freshwater gastropod *Latia neritoides* is endemic to the streams of New Zealand's North Island. This species has evolved a unique defence system: it exudes a luminescent mucus thought to deter predators. While the bioluminescence itself has been investigated before, the underlying gland system has remained unstudied and relevant information to understand the defence system has been missing till now. For the release of the glowing mucus of *L. neritoides* two places of origin were assumed: the lateral foot area or the mantel cavity. In this study the focus was on the first suggestion. To gain insight into the defence system, morphological as well as histochemical analyses were performed involving all secretory gland types in the sub-epithelial foot layer. The results were compared with the foot gland system of *Neritina* sp., a snail living in a comparable habitat, but using a different survival strategy. The gland types of the two gastropods were compared and their mucus types were investigated. Seven subepithelial gland cell types can be distinguished in the foot region of *L. neritoides*. *Neritina* sp., in contrast, has six gland cell types of which three laterally located ones are epithelial. Both species show a pedal gland in the anterior foot region. A striking difference between the species are two prominent subepithelial gland cell types (L1l/L2l) in the lateral foot area of *L. neritoides,* which are missing in *Neritina* sp. These gland cells are distributed throughout the entire lateral foot area of *L. neritoides* and make up about 85% of the mucus gland cells in this area. Defence mucus and trail mucus of *L. neritoides* show different specificities in lectin staining, but are not equally represented in the gland cell types. Yet, based on the huge size and high density of L1l and L2L, we envision a role for these gland types in the defence system.

1. Introduction

Gastropods include numerous, diverse clades (Bouchet et al., 2017) that colonized almost all habitats ranging from marine and intertidal habitats, limnic ponds, rivers and caves, to terrestrial habitats like rainforests and alpine areas (Morris and Taylor, 2000). All gastropods release mucus of different consistency serving a multitude of purposes. Mucus can be a fluid hydro-like gel released for crawling or to overcome sharp objects in case of land snails (Denny, 1983). Alternatively, mucus can harden when it is released to adhere the animal to leaves or save them, in case of the Euconulids, from dehydration (Barrientos, 2020). Limpets use their mucus to glue themselves to the substrate and to prevent themselves from getting washed away from their habitat in the intertidal zone (Bingham, 1972; Smith et al., 1999). As there are so many different functions of the mucus, it seems only reasonable to assume that there are various specific glands and gland cell types involved in the synthesis and release of distinct and interacting components of the mucus.

Enhanced substrate adherence in various marine snails brought their pedal mucus secretions into the focus of science (Chapman and Underwood, 1996; Smith, 2002, 1992; Smith et al., 1999). However, the morphological and histochemical characterisation of mucus glands and

* Correspondence to: Department of Evolutionary Biology, University of Vienna, Djerassiplatz 1, A-1030 Vienna, Austria.
E-mail address: gerhard.steiner@univie.ac.at (G. Steiner).

https://doi.org/10.1016/j.zool.2022.126067
Received 4 March 2022; Received in revised form 28 November 2022; Accepted 20 December 2022
Available online 22 December 2022

their components, *i.e.* the gland cells, has largely been neglected. To date, only a few species have been studied in this regard. *Patella vulgata* has nine pedal gland cell types (P1–9) (Grenon and Walker, 1978). The glands can be separated into six main types (P1, P2, P5, P6, P8, P9) that secrete mucus on the ventral side, and three (P3, P4, P7) that secrete mucus on the lateral side of the foot. Four frequently present gland types located on the sole (P2, P5, P8, P9) secrete acidic mucopolysaccharides with sulphated and non-sulphated sugars and also neutral mucopolysaccharides. No proteins were detected in these gland types (Grenon and Walker, 1978). Gland types P2, P5, and P8 are subepithelial gland cells secreting adhesive mucus. Type P9 is described as an epithelial mucocyte. Here, weakly acidic mucopolysaccharides were detected, and it was presumed that this mucus type served for lubrication (Grenon and Walker, 1978). Calcium was not detected in any of the gland cells. The two less common gland cell types, P1 and P6, by contrast, contain proteins (Grenon and Walker, 1978). P6 is a slender gland cell type of low abundance on the sole of *P. vulgata.* P1 consists of clustered cells and secretes into a groove situated at the outer area of the sole, suggesting a function in connection with locomotion of the animal. In the second investigated species, *Acmaea tessulata*, comparable gland types were detected (Grenon and Walker, 1978).

Further studies on limpet-like molluscs by Lee et al. (1999) involved the secretory cell types, or mucocytes, of five abalone species (*Haliotis gigantea, H. sieboldii, H. discus, H. discus hannai, Sulculus diversicolor aquatilis*), which were compared with each other. One and two gland cell types were identified in the lateral foot area and ventral foot area, respectively. One ventral mucocyte is epithelial and secretes acidic or neutral mucosubstances, whereas the other is subepithelial and secretes a combination of neutral and acidic mucosubstances. The lateral mucocytes contain both (neutral/acidic) mucosubstances.

Chaparro et al. (1998) found four mucocyte types (M1-M4) in the ventral foot area of *Crepidula dilatata*, of which only M4 is subepithelial and reported more abundant in older, female individuals. These individuals are sessile and M4 is suspected to be responsible for adhesion, whereas the other epithelial mucocytes are thought to promote locomotion. No histochemical data were provided.

The limpit-like *Latia neritoides* Gray, 1850 is one of three extant species of the family Latiidae in the clade Hygrophila, all endemic to the rivers of the North Island of New Zealand (Bowden, 1950; Meyer-Rochow and Moore, 1988). This freshwater gastropod has the unusual ability to release a greenish glowing mucous secretion when disturbed or attacked by predators, such as the dobsonfly *Archichauliodes diversus* larva (Corydalidae), or the eels *Anguilla dieffenbachii* and *A. australis* (Meyer-Rochow and Moore, 1988). It is suggested that this sudden light emission and the sticky, glowing mucus repel and confuse predators and make them conspicuous to their own predators, especially during the night or in low-light environments (Meyer-Rochow and Moore, 1988). Similar abilities and behaviour are reported from other aquatic and terrestrial animals in a defence system context, *e.g.* Annelida (Verdes and Gruber, 2020), although experimental confirmations seem to be difficult.

Bioluminescence is unknown in the sister group to Latiidae, the South American Chilinidae (Ovando and Gregoric, 2012). As the limpet-shaped shell of *Latia neritoides* provides protection against mechanical assaults, the additional defence component of the luminescent mucus is unexpected (Meyer-Rochow and Moore, 1988) and raises the question on the differences of the glandular system in this species in relation to that of other gastropods with a similar shape living in similar habitats, but lacking the luminescent mucus.

Non-limpet like species of the genus *Neritina* (Neritimorpha) live in comparable habitats (Baker, 1923) and are easy to access and examine because they are popular gastropods for aquaria. Like most shell-bearing gastropods, *Neritina* sp. can close its shell with the (here calcified) operculum when attacked, and therefore a chemical defence mechanism is not needed (Vermej, 2015). *Neritina* species reach 40 mm in shell length (Abdou et al., 2017), which is a huge benefit for sampling of their trail mucus, compared with the much smaller *L. neritoides* (11 cm in length) (Ohmiya et al., 2005).

To date, research on *Latia neritoides* has focused mainly on the glowing mucus. It is known that for the bioluminescence of its presumed defence mucus (emission maximum near 505 nm; Meyer-Rochow and Moore, 1988) the following components are needed: the *L. neritoides* luciferin with an emission of a yellow-greenish light, the luciferase, a so-called purple protein which is a red-fluorescent protein (38 kDa), and oxygen (Shimomura, Johnson, and Kohama, 1972; Shimomura and Johnson, 1968a, 1968b). Two candidate regions of origin of the glowing mucus are mentioned: the lateral foot area (Bowden, 1950) or the mantle cavity, the latter implying the release through the pneumostome (Meyer-Rochow and Moore, 1988).

A considerable amount of research has been carried out on bioluminescence in general (Anctil, 2018; Haneda, 1985; Harvey, 1952; Meyer-Rochow and Moore, 2009; Ramesh and Meyer-Rochow, 2021; Shimomura and Yampolsky, 2019; Wilson and Hastings, 2013), but specifically with regard to gastropods much less is known about their luminescence and how their ability to produce and emit light has evolved (Yu et al., 2018).

Hinea brasiliana (Planaxidae), native to rocky shorelines of New Zealand and Australia, is one of the few known gastropods using bioluminescence (Deheyn and Wilson, 2011; Ponder, 1988). *Melanella* spp. (Marshall, 1997) and *Angiola* spp. (Oba and Schultz, 2014) are other marine bioluminescent species of gastropods. In *H. brasiliana* the bluish-green light is known to be produced in the epidermal cells on the mantel cavity roof and flashes, when the animal is disturbed (Deheyn and Wilson, 2011).

Quantula striata is the only land snail known for bioluminescence and it has been speculated that its bioluminescence is used for communication (Counsilman and Ong, 1988). In *Quantula* an organ, which is part of the suprapedal gland, produces yellow-greenish light (Counsilman et al., 1987), but no luminescent components are actively secreted (Isobe et al., 1991).

This study focuses on the characterisation of the gland cell types of the *Latia neritoides* pedal system and a comparison with the foot of a non-glowing gastropod and its mucus (*Neritina* sp.). An elucidation of the two species' gland morphologies and differential reactivities based on specific histochemical reactions, as well as a comparison of tissues and secreted mucus types, are expected to help in differentiating between defence and trail mucus-producing glands.

2. Material and methods

2.1. Study site and species

Adult specimens of *Latia neritoides* (n = 242) were collected in a freshwater river next to Kawhia (S 38°05.680′ E 175°06.522′) on the North Island of New Zealand during two sampling trips (2019, 2020) under a Department of Conservation *Te Papa Atawhai* sampling permit (70757-RES). The animals were sectioned and fixated for morphological analyses at ultrastructural (n = 2) and histochemical (n = 12) levels directly after collection. Two specimens were frozen and later freeze-dried for scanning electron microscope (SEM) imaging and gland element analyses. Additionally, four animals were fixated in 96% EtOH for DNA-based identification. The remaining specimens (22) were only collected for mucus harvesting (see below) and released again to their natural habitat within 2 days.

Adult specimens of *Neritina* sp. (n = 18) were bought at a pet store in Vienna and kept under lifelike conditions in a freshwater aquarium. Prior to fixation, all animals were used for mucus collection. Two individuals were sectioned and fixated for ultrastructure morphology analysis, and three for histochemical analysis. One specimen was freeze dried and submitted to SEM and elemental analyses. Six individuals were fixed in 96% EtOH for DNA-based identification. The remaining specimens (n = 6) were kept only for mucus collection.

Species identification was performed on molecular basis. DNA was extracted with DNeasy Blood & Tissue Kit (Qiagen, Hilden, Germany) according to the manufacturer's protocol. For amplification of CO1 the primers LCO1490 (GGTCAACAAATCATAAAGATATTGG) and HCO2198 (TAAACTTCAGGGTGACCAAAAAATCA) were used. ArcticZymes (A'SAP method) enzymes (ArcticZymes Technologies ASA, Norway) were used for cleaning up the PCR product before it was sent to Microsynth Austria GmbH for sequencing. Accession numbers of the obtained sequences and of other taxa used in the phylogenetic analyses are listed in Supplement Table 1. Sequence quality checks were made with FinchTV 1.4.0 (Geospiza Inc.). Sequences alignment and model selection was done in GeneDoc 2.7.0 (Nicholas and Nicholas, 1997) and MEGA X (Kumar et al., 2018). MrBayes 3.2.4 (Ronquist and Huelsenbeck, 2003) was used for Bayesian Inference, with 2 × 4 chains and 5 million generations, and a visually/manually determined burnin. Trees were generated with Figtree 1.4.3 (Rambaut, 2010). The species identity of the *Neritina* sp. specimens is not unequivocally resolved (see supplement Fig. 4).

2.2. Mucus collection

Latia neritoides were kept in freshwater tanks for 1–2 days. To obtain an almost pure sample, the animals were gently cleaned with a soft toothbrush and then poked with a plastic toothpick to stimulate them to release the luminescent defence mucus. This mucus type was deposited with forceps on a glass slide or a standard SEM stub (Greistorfer et al., 2020) and air dried at room temperature. To obtain samples of the trail mucus the animals were kept overnight in 50 ml plastic tubes (with a hole in the lid in an air-gassed freshwater aquarium), which were internally lined with ACLAR® fluoropolymer film (Science Service, Munich, Germany). Afterwards the foils were isolated and air-dried at room temperature under clean conditions. All handling was performed with gloves and the animals were released directly afterwards to their natural habitat. Trail mucus samples of *Neritina* sp. were collected repeatedly from each animal in an interval of two weeks to ensure that the animal had time to regenerate, and stored in the same way as for *L. neritoides*.

2.3. Gland morphology

For ultrastructural analyses with the transmission electron microscope, specimens of *L. neritoides* and *Neritina* sp. were processed as described in Greistorfer et al. (2020). For the reconstruction of the gland types L1l and L2l in *L. neriotoides* the section thickness was reduced to 0.5 µm. For *L. neritoides* the fixation (2 hrs.) was completed in New Zealand while post-fixation and embedding was performed at the University of Vienna in Austria, together with the *Neritina* sp. samples. Ultrathin sections of both species were stained with Richardson solution and uranyl acetate. For scanning electron microscopy, samples of both species were frozen in cryo tubes with dry ice (*L. neritoides*) and liquid nitrogen (*Neritina* sp.) and subsequently freeze-dried with a vacuum freeze dryer (Christ Beta-RVC) at the research institute NIWA (National Institute of Water and Atmospheric Research) in Hamilton, New Zealand (*L. neritoides*) or a freeze dryer Christ Alpha 1–4 LSC at the department for Division of Terrestrial Ecosystem Research in Vienna, Austria (*Neritina* sp.). The freeze-dried samples were cut into cross sections with an ultra-microtome blade MS 100 (Micros Austria) and attached with double tape carbon foil on aluminium stubs. Afterwards the samples were coated for 120 s with a gold layer in a sputter coater (JEOL JFC-2300HR). Observations were performed on a scanning electron microscope (JEOL IT 300 LaB6 LV, Jeol Germany GmbH) at 20 kV.

2.4. Histochemistry of tissue and mucus

Specimens of *L. neritoides* were fixed in Bouin (Aescht et al., 2010) or Carnoy's solution (Kiernan, 1999) and specimens of *Neritina* sp. were fixed in acetic-alcohol-formalin (Aescht et al., 2010) and Carnoy's solution (Kiernan, 1999) and then were serial-sectioned at 5–7 µm, following Greistorfer et al. (2020). The histological and histochemical evaluations were performed with native mucus samples as well as paraffin sections. Staining protocols followed those described in earlier work (Greistorfer et al., 2017), with the following modifications: Alcian blue G8X at the pH level of 1.0 (Aescht et al., 2010) was additionally combined with Azan trichrome (Böhm and Oppel, 1919) to visualise the gland types in detail with the surrounding muscle net; Safranin – O staining was excluded in the present study because no added value was expected from it. Abbreviations used for the staining solutions: Periodic acid Schiff staining: PAS, Alcian blue G8X: AB, Biebrich scarlet: BS, Toluidine blue O: Tol-O.

2.5. Lectin affinity tests

We applied 24 fluorescence-labelled lectins (Table 2 for details) on mucus samples for a detailed description of the sugar moieties, following von Byern et al. (2021). The dried mucus samples were re-hydrated for 10 min at room temperature in phosphate buffered saline (PBS, 0.1 M, pH 7.4) and then incubated with lectin at a dilution of 1:500 for one hour following the manufacturer's protocol. Subsequently, the mucus samples were washed five times in 0.1 M PBS and mounted with Fluoromount-G™ mounting medium (Thermo Fisher Scientific). For negative controls and to check autofluorescence no lectin was added to the sample and the mucus samples only washed with 0.1 M PBS and mounted. In the case of a positive affinity result of a specific lectin, paraffin sections were used to confirm the reactivity of the lectin in the tissue sample. For this the paraffin sample was deparaffined in 100% xylol and hydrated isopropanol (100%) and degrading in ethanol series (100%, 90%, 80%, 70%) and distilled water. Subsequently the samples were washed 3 times in 0.1 M PBS for 10 min and 3 times in 0.1 M PBS + 1% Triton X for 10 min. Then the samples stayed in 5% BSA in 0.1 M PBS + 1% Triton X for 10 min, were washed again with 0.1 M PBS + 1% Triton X (10 min) and were incubated with different lectins (Table 2 for details). After incubation with lectins for one hour, the samples were again washed 3 times in 0.1 M PBS in 1% Triton X and then they had a bath 3 times in 0.1 M PBS each for 10 min. The same mounting medium was used as for the mucus samples.

2.6. Element analysis of tissue and mucus

EDX-measurements of the mucus were made as described in Greistorfer et al. (2020). We performed element analysis on the freeze-dried tissue sections before gold coating. We used an EDAX Ametek Octane plus detector on an electron scanning microscope (JEOL IT 300 LaB6 LV, Jeol Germany GmbH) and analysed using Team Software (version 4.3). Mucus and control samples (water, aluminium stubs) were measured at 20 kV, tissue at 15 kV. Point measurements were only taken for single granules (collecting time 30 s). All mucus samples were investigated with dot mappings, with a collecting time from 686 s up to 2018 s. All values reported are atom % (at%), the detection limit was 0.1 at%.

2.7. Visualisation, reconstruction and measurements

Secondary and backscattered electron image data were combined and processed with Photoshop CS6 (Adobe Systems, San Jose) for colorization of the SEM pictures. Together with Illustrator CS6 (Adobe Systems, San Jose), this program was also used to create schemes of the detected gland cells and their distribution in the animals based on histochemical and ultrastructural investigations.

The muscle network surrounding the glands in the lateral area of *L. neritoides* was visualised by a reconstruction of this area from semithin serial sections (0.5 µm). The pedal gland Lpg was reconstructed from serial paraffin Section (5 µm). Both reconstructions were done with Amira (Thermo Scientific). Measurements of glands (only with a visible

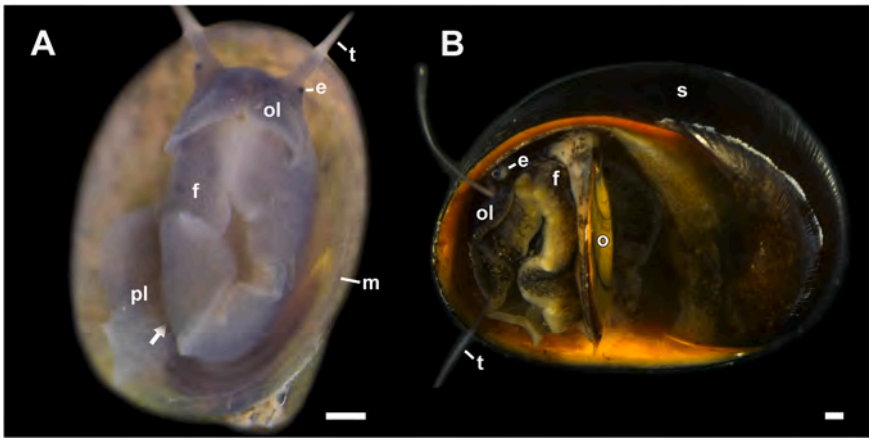

Fig. 1. Ventral views of (A) *Latia neritoides* and (B) *Neritina* sp. with a partly curled foot. Gland cells of foot (f), mantle (m), oral lobes (ol) and pneumostomal lobe (pl) are shown. An arrow marks the pneumostome in (A). Additionally labelled: e = eye, o = operculum, s = shell, t = tentacle. Scale bars in all images = 1 mm.

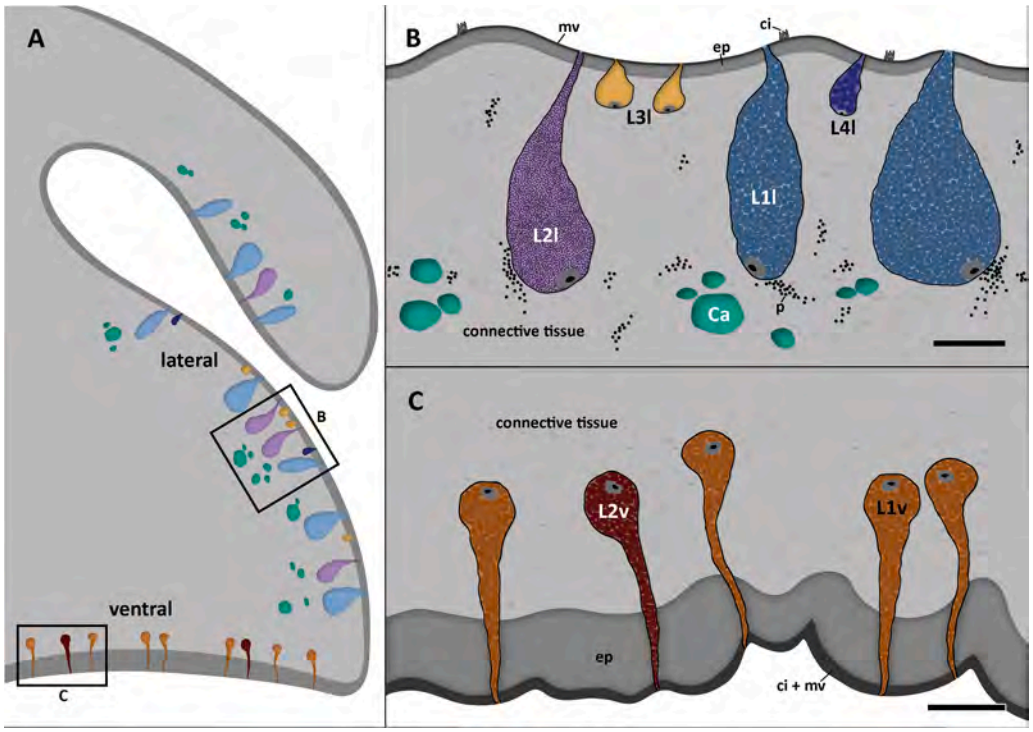

Fig. 2. Schematic overview and detailed visualisation of the pedal gland system in the foot of *Latia neritoides*. (A) Distribution pattern of the different gland cell types. (B) Detailed localisation and granular content of the lateral (L1l-L4l, L1l = blue, L2l = violet, L3l = yellow, L4l = dark blue) and (C) the ventral (L1v = orange, L2v = red) gland cell types. The lateral as well as ventral epithelia (ep) are covered with microvilli, thicker ventrally than laterally, and their granules as well as the different distribution patterns of their cilia (ci) and microvilli (mv) are apparent. Calcium deposits (Ca = turquoise) and pigments (p) are given in the subepithelial lateral area. Scale bar in image B 25 μm, in image C 100 μm.

open duct) and epithelia were performed on semithin sections (0.5 μm/1 μm). Granules were measured on ultrathin sections of 60 nm thickness. Reported values are arithmetic means of 10 replicate measurements.

2.8. Terminology

The terminology of the gland cells and gland areas follows that of Greistorfer et al. (2017) and von Byern et al. (2018): the first letter indicates the taxon (L for *Latia*, N for *Neritina*), followed by the number of the gland cell type and the body region (l for lateral, v for ventral).

3. Results

The investigated areas comprise the ventral and lateral foot region in both species and the pneumostomal lobes in *Latia neritoides* (Fig. 1A, B).

3.1. Latia neritoides

The thickness of the epithelial layer of the foot increases from lateral (9 μm) to ventral (14 μm) (supplemental Fig. 1A-E, Figs. 2A-C, 3C). The ventral epithelium is uniformly ciliated (supplemental Fig. 1C, E, Fig. 2C), but cilia appear in clusters on the lateral sides of the foot (supplemental Fig. 1D, Fig. 2B). The lateral foot epithelium is pigmented (supplemental Fig. 1B, Figs. 2B, 5B, 7B) and shows calcium deposits (Ca) (Figs. 2B, 8B) below the mucus glands.

The lateral foot area (Fig. 2B) contains four subepithelial gland cell types (L1l, L2l, L3l, L4l), whereas the ventral area (Fig. 2C) has only two subepithelial gland cell types (L1v, L2v).

The gland types L1l and L2l are equally distributed throughout the lateral foot area and sum up to 80–90% of all glands in this area. Gland types L3l and L4l are less abundant and account for only 10% and 5%, respectively. In the ventral area, L1v represents 80% of all the glands, whereas L2v accounts for the remaining 20%.

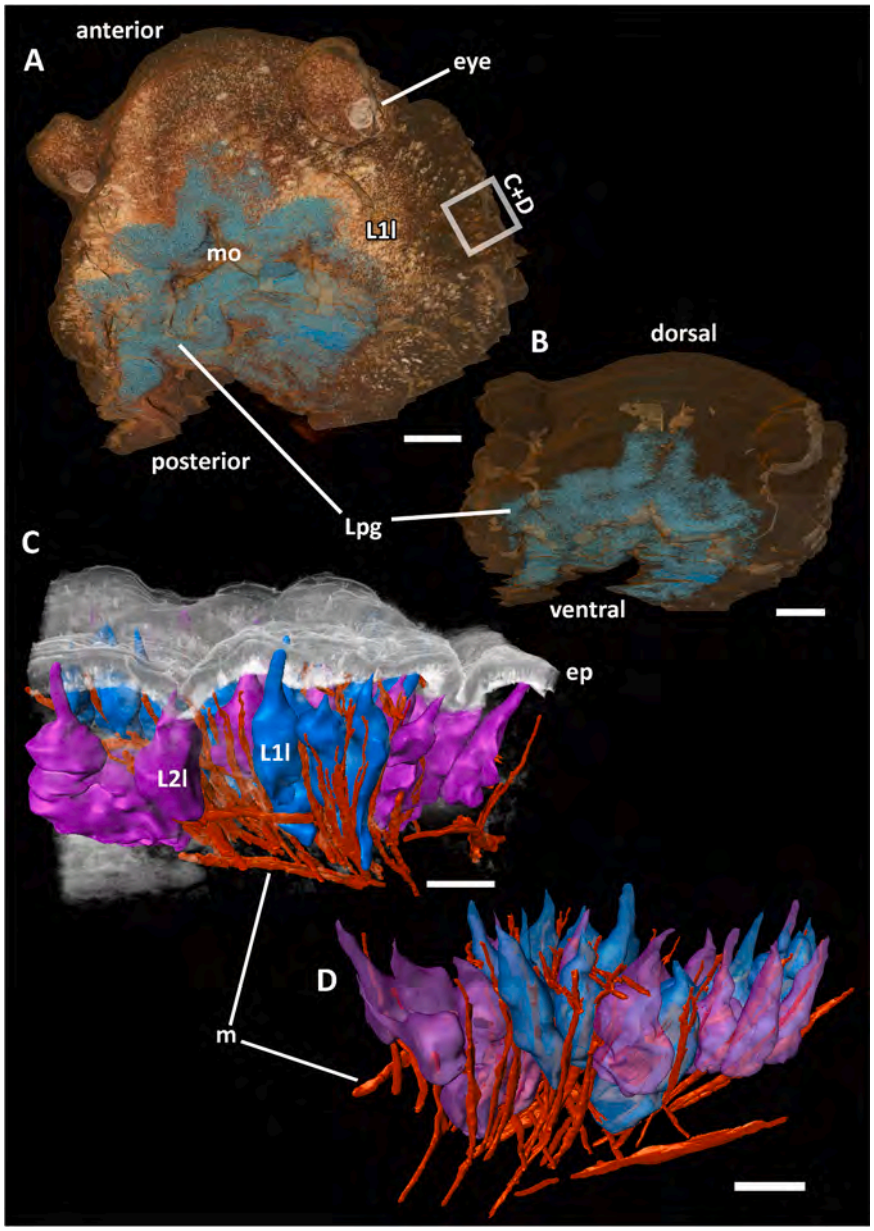

Fig. 3. 3D reconstructions of the anterior foot region in *Latia neritoides*. (A, B) Localisation of the pedal gland (Lpg = *Latia* pedal gland, = light blue) surrounding the mouth opening (mo). (C, D) Detail of the lateral area with partly reconstructed muscle net (m, coloured in red) and the gland cell types L1l (blue) and L2l (violet) beneath the epithelium (ep, coloured in white). Scale bars in image A and B 400 μm, in image C and D 40 μm.

In the ventral area L1v is 4 times more abundant than L2v (Fig. 2A). The nuclei are located in the basal parts of all gland cell types (supplemental Fig. 1A, B, Fig. 2A, B, C, 4A, B, E). A densely packed gland area (Lpg) is located in the anterior region of the foot (Fig. 3A, B, 7A, B, C, D). The foot muscle network surrounding all lateral and ventral gland cell types (supplemental Fig. 1C, Fig. 5C) is visualised for the lateral area (Fig. 3C, D). However, no direct functional connection to the gland cells can be observed.

3.1.1. *Gland morphology*

The gland cell type L1l has a bag-like shape and is commonly present in the lateral area of *L. neritoides* (Fig. 2B). The dimension of L1l varies depending on the area and expands from the epithelium surface to a depth of 146 μm. The gland cell type is filled with spherical vesicles ranging from 2 to 7 μm in diameter (supplemental Fig. 1A, B, D; Fig. 4B), which fuse before release (Fig. 4C). The gland cell type L2l resembles in size and shape those of L1l but differs in contents. The material is finely granulated (supplemental Fig. 1A, B, D; Fig. 4A) and shows no modification during release (Fig. 4D). Nevertheless, variations related to the electron density of the gland content are noticeable (Fig. 4A). Gland cell type L3l is less common, smaller in size (26 μm) (Fig. 2B) and contains fine granulated material (supplemental Fig. 1A, B, Fig. 4E). The last lateral gland cell type L4l is least abundant in the lateral foot area. It compares in size (23 μm) to L3l (Fig. 2B), but contains round and uniformly spherical electron dense vesicles of variable size (1–3 μm) (supplemental Fig. 1B; Fig. 4B).

The ventral gland cell type L1v (Fig. 2C) has a length of 159 μm and crosses the foot epithelium as a narrow duct containing / releasing finely granulated material (Fig. 4G). Upon release, the gland content consists of more or less roundish, densely packed vesicles (0.6–1 μm), which reveal a striated/dotted pattern of more and less electron dense areas inside the vesicles (Fig. 4F, G).

The gland cell type L2v (Fig. 2C) is of similar size and shape as L1v. Its contents consists of uniformly shaped vesicles 0.8–1.5 μm in diameter

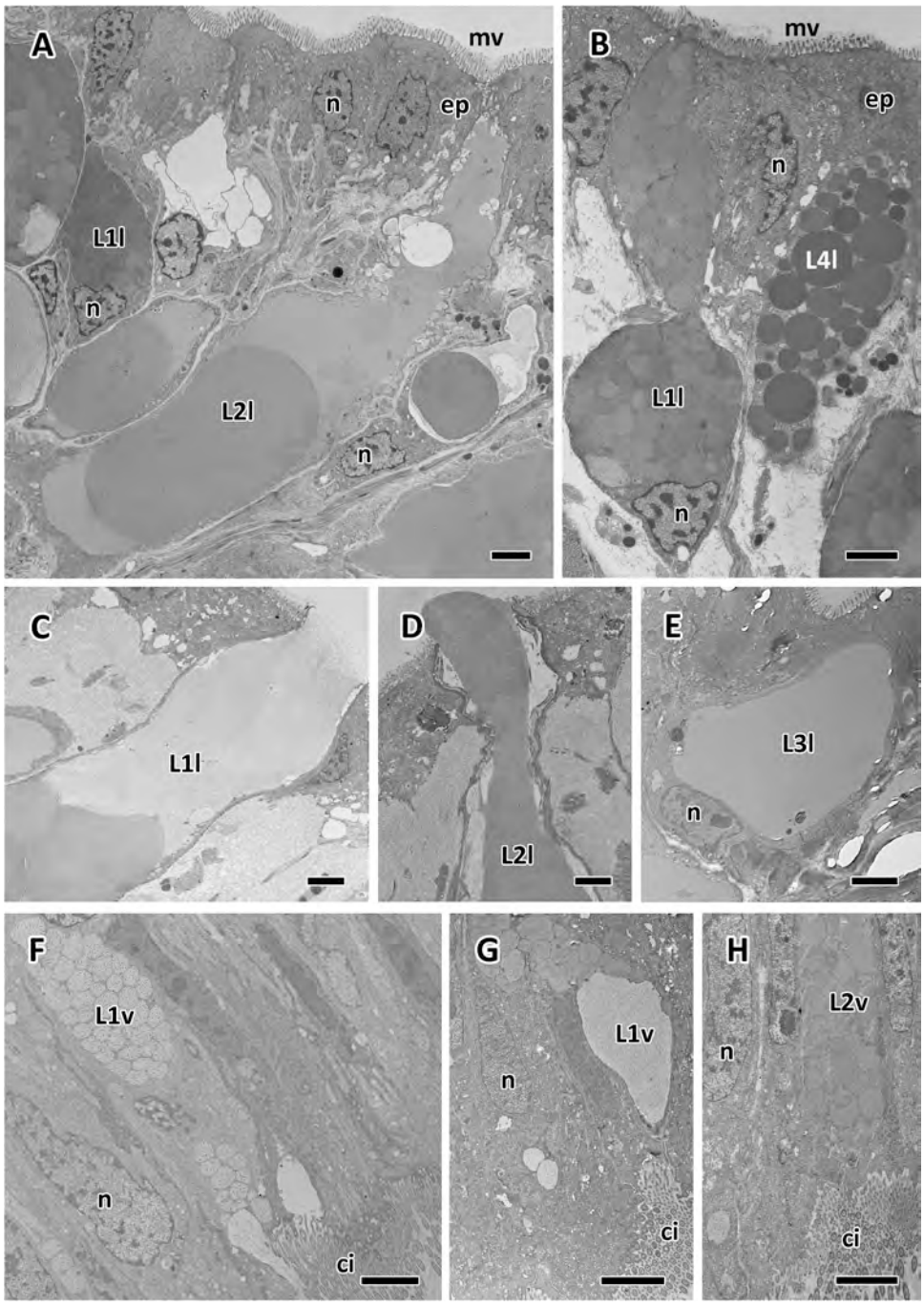

Fig. 4. Ultrathin images of the pedal gland types in *Latia neritoides*. (A, B) In all gland cell types, the nucleus (n) is located basally, and a microvilli (mv) layer is present. (A) The granular content of L1l contains roundish vesicles while in L2l smooth granulated material with different electron density could be observed. (B) In contrast to L1l the vesicles of L4l are spheroid and electron dense and of different size to each other (1–3 μm). (C) Apically the vesicles of L1l dissolve to a finely-grained material before secretion. (D) Emission of gland content of L2l. (E) The granular material of L3l is uniform and fine grained and could not clearly be differentiated from L2l. The nucleus is situated basally (n). (F – H) Ventrally a ciliated layer is present. (F) The vesicles of L1v show a striated/dotted pattern of more and less electron dense areas, (G) fusing apically. (H) The granular material of L2v is of uniform electron density; a fusion of granules at the release site could not be observed. Scale bars in all images 2.5 μm.

(supplemental Fig. 1C, E; Fig. 4H). A release of vesicles was not observed.

The pedal gland Lpg (Fig. 3A, B, 7A, B, C, D) incorporates a content (0.6–3 μm in diameter) similar to that of L1v (Fig. 7C, D), but the Lpg gland cells are considerably more bulky (Fig. 7B).

3.1.2. *Histochemistry and lectin affinity of the lateral and ventral glands*

Gland cell type L1l showed a strong positive reaction to PAS (Fig. 5B), Alcian blue at both pH levels, Toluidine Blue as well as to the combination of Alcian blue and PAS (Fig. 5A, Table 1) indicating the presence of sulphated (Alcian blue pH 1.0) and carboxylated glycoproteins (Alcian blue pH 2.5). Other stains such as Biebrich scarlet (all pH levels), Calcium-related stains (von Kossa and Alizarin Red S) and Arnow stain (to locate the presence of L-DOPA) were negative. The lectin affinity tests gave a positive reaction to N-acetyl galactosamine (VVL, GSL1) (Fig. 6A, B, E) and α-linked fucose (UEA1) (Table 2) in this gland cell type. In L2l none of the tested histochemical staining showed a positive reaction (Fig. 5A, B, Table 1), however, presence of N-acetyl galactosamine (VVL, WGAs, WGA) (Fig. 6C), mannose linked sugar moieties (GNL) and galactose linked to N-acetyl galactosamine (JAC) (Table 2) could be confirmed. For the gland cell type L3l it was not possible to differentiate it from smaller parts (as ducts) of L1l, and L4l was not visible in paraffin sections at all.

L1l, L1v and Lpg contained sulphated and carboxylated glycoproteins (Fig. 7B, Table 1), whereas in L1v a weaker reaction to PAS staining than that seen in L1l (Table 1) was obtained. Again, no reaction occurred in connection with the other tested staining methods. The contents of L1v showed a positive affinity to a number of sugar moieties as mannose

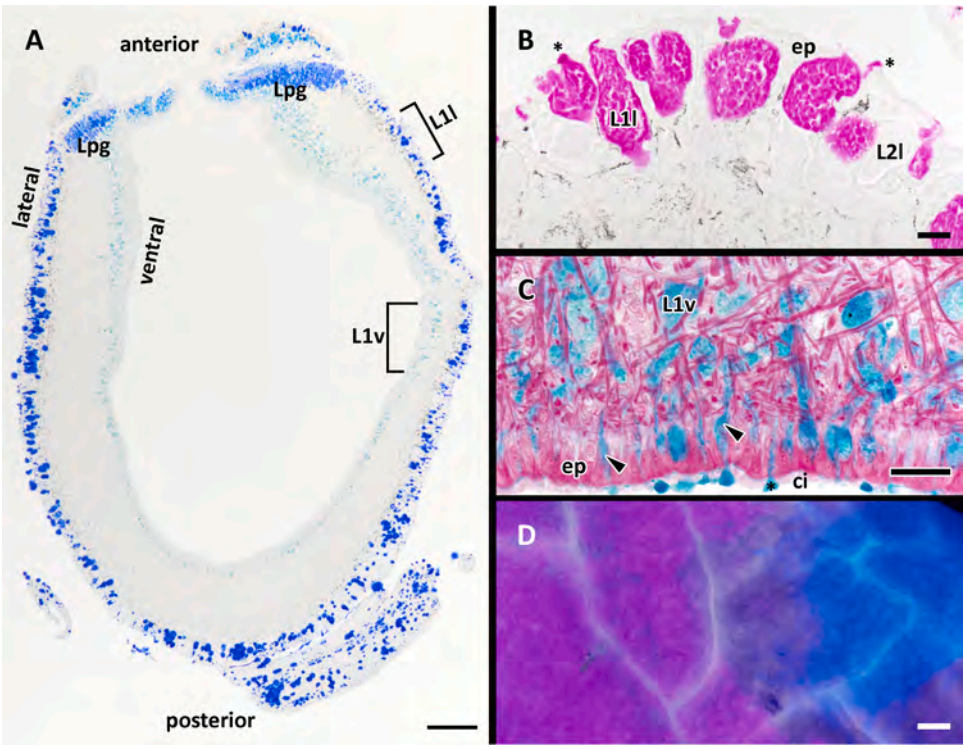

Fig. 5. Staining result of the pedal glands in *Latia*. (A) Localisation of L1l, L1v and *Latia* pedal gland (Lpg) in a cross section of the foot. All gland types show a positive reaction to periodic acid-Schiff – Alcian blue (PAS-AB) staining at pH 1.0. (B) The strong positive reaction of L1l and its released content (black asterisks) to PAS staining is indicative of the presence of carbohydrates, while L2l is negative. (C) In the ventral area the combination stain of Azan and Alcian blue at pH 1.0 shows the arrangement of the muscles surrounding the gland cell and its duct (black arrowhead). In L1v gland cell, duct and secreted content (black asterisk) are reacting positive to sulphated mucosubstances, while the epithelium (ep) remains unreactive. (D) Sulphated glycoproteins (Alcian blue at pH 1.0 combined with PAS) are not homogeneously dispersed in the defence mucus; on the left side the purple PAS stain is apparent, while on the right a strong blue Alcian blue reaction could be observed. Additionally labelled: ci = ciliated layer. Scale bar in image A 400 μm, in image B and C 25 μm and in image D 50 μm.

(GNL), α-linked mannose (ConA), N-acetyl galactosamine (VVL, WGA, WGA's, GSL1, SBA, LEL), galactose linked to N-acetyl galactosamine (PNA, JAC) (Fig. 6F, Table 2). For Lpg an affinity to α-linked mannose (ConA), to N-acetyl galactosamine (VVL, GSL1, GSL2) as well as to α-linked fucose (UEA1) is confirmed (Fig. 6D, E, Table 2). A differentiation between L1v and L2v was not possible in the stained paraffin sections.

3.1.3. Histochemistry and lectin affinity of the two mucus types

In contrast to the identified gland types, both mucus types (defence and trail) also showed a positive staining reaction to basic proteins (Biebrich scarlet at all pH levels) and calcium (von Kossa staining). As in the glands, sulphated, carboxylated glycoproteins (positive Alcian blue, PAS and Toluidine blue staining) were present (Fig. 5D). However, differences are apparent in regard to the characteristics of its sugar moieties: the trail mucus exhibits strong affinities to WGA and ConA, but the defence mucus reacts also positive to VVL, WGAs, GSL1, PNA, and SNA1, but only weakly on WGA (Table 2). Both mucus types tested positive for lipids (Sudan black B).

3.1.4. Element analysis of tissue and mucus

In both mucus types (trail/defence) the EDX measurements revealed a high concentration of sodium (trail 0.82 at%; defence 1.13/0.99 at%) and chlorine (trail 0.87 at%; defence 0.75/0.79 at%). A difference between them was notable with regard to the sulphur concentration, which was higher in the defence mucus (trail 0.87 at%; defence 0.41/0.39 at%) and also contained potassium (0.15/0.19 at%) (Fig. 8D, Table 3). In contrast, silicon could be detected in the trail mucus (0.17 at %). The defence mucus was collected in two consecutive summer terms (2019/2020), and results from both years were nearly identical. Elemental calcium, magnesium and phosphorus could also be detected, although in smaller amounts (Table 3). It was possible to investigate the two prominent gland cell types in the lateral area (Fig. 8A, B, C). The gland cell type L1l has a high proportion of magnesium (0.45 at%) and phosphorus (0.62 at%), whereas in L2l the sulphur concentration (0.46 at%) stands out. With this method it was also possible to identify calcium deposits, situated next to the lateral gland area (Fig. 8C). Here a high amount of calcium (5.65 at%), magnesium (1.85 at%) and fluorine (0.19 at%) was detectable (Table 3). Copper was neglected, because the stubs' content could render the results unreliable.

3.2. Neritina sp

As in *L. neritoides,* the ventral epithelial foot layer in *Neritina* sp. is thicker (20 μm) than the lateral layer (14 μm) (supplemental Fig. 2A, B, C, D, E, F, Fig. 9A) and more uniformly ciliated (supplemental Fig. 2A, D, E, F, Fig. 9B, C; 10C, D, E, G, H). The pigmentation of the lateral foot epithelium alternates between black and brown. Ventrally only black pigments were present (Fig. 9B, C; 10A, B, C).

The lateral pedal epithelium in *Neritina* sp. differs from that of *L. neritoides* by showing three epithelial gland cell types, N1l-N3l (Fig. 9A, B). The two gland cell types in the ventral epithelium (N1v, N2v) are subepithelial and all of them have basally located nuclei (Fig. 9A, B, C; 10A). The most abundant gland cell type in the lateral area is N1l (50%), followed by N2l (45%) and N3l (5%). A gland-cell-like structure is observed in this area as frequent as N2l, but neither a nucleus nor a duct leading through the foot epithelium are evident. Therefore, this structure is considered a storage (Ns), although it is unclear what kind of substance it might store (Figs. 9B, 10E).

In the ventral foot area N1v is found 4 times more often than N2v (Fig. 9A, C). Both gland cell types may extend to 220 μm under the foot epithelium.

Between the lateral and ventral area, a big pedal gland (Npg) (730 μm) is present in the anterior edge of the *Neritina* sp. foot (supplemental Fig. 2E, Fig. 9A).

3.2.1. Gland morphology

The most abundant gland cell type in the lateral epithelium N1l has a bulbous outline or shape and contains densely packed vesicles of 1–2 μm in size that possess a dotted electron dense and translucent pattern (Fig. 10A, B). Following the releases of its vesicles, they transform into merged fine-grained material (Fig. 10A, B). The less abundant N2l appears more slender, containing mostly electron dense vesicles (1–1.5 μm) and resembling N1l in relation to its discharge (Fig. 10A).

Table 1
Histochemical comparison of the different mucus and gland cell types of *Latia neritoides* and *Neritina* sp. Staining type, the staining acronym and the specificity are listed. The reaction for each staining method for the different secretions and gland cell types is indicated by: ++ = strong positive reaction; + = positive reaction; +- = weak reaction; - = no reaction; n.d. = not differentiable; n.v. = not visible; n.s. = not stained.

mucus				gland cell types							mucus		gland cell types				
Staining	Specificity	*Latia neritoides* defence mucus	*Latia neritoides* trail mucus	L1l	L2l	L3l	L4l	Lv1	L2v	Lpg	*Neritina* sp. trail mucus	N1l/ N2l	N3l	Ns	N1v	N2v	Npg
PAS negative	–	–	–	–	–	n. d.	n. v.	–	n. d.	–	–	–	n. d.	–	–	n.d.	–
Alcian Blue pH 1.0	Sulphated Mucosubstances	+	+	++	–	n. d.	n. v.	++	n. d.	++	+	+	n. d.	–	+-	n.d.	++
Alcian Blue pH 2.5	Sulphated & Carboxylated Mucosubstances	+	+-	++	–	n. d.	n. v.	++	n. d.	++	+	+	n. d.	–	+-	n.d.	++
Alcian Blue pH 1.0 + PAS	Sulphated Glycoproteins	+ coloration not homogeneous	+ coloration not homogeneous	++	–	n. d.	n. v.	+	n. d.	++	+	+	n. d.	–	+-	n.d.	+
Alcian Blue pH 2.5 + PAS	Sulphated & Carboxylated Glycoproteins	+ coloration not homogeneous	+ coloration not homogeneous	++	–	n. d.	n. v.	+	n. d.	++	+	+	n. d.	–	+-	n.d.	+
Toluidin Blue pH 4.5	Acidic Proteins	+	+-	+	–	n. d.	n. v.	+	n. d.	+	+	–	n. d.	–	+	n.d.	+-
Biebrich Scarlet pH 6.0	Basic Proteins	+	+	–	–	n. d.	n. v.	–	n. d.	–	+	–	n. d.	–	–	n.d.	–
Biebrich Scarlet pH 8.5		+	+-	–	–	n. d.	n. v.	–	n. d.	–	+-	–	n. d.	–	–	n.d.	–
Biebrich Scarlet pH 9.5		+-	+	–	–	n. d.	n. v.	–	n. d.	–	+-	–	n. d.	–	–	n.d.	–
Biebrich Scarlet pH 10.5		+	+-	–	–	n. d.	n. v.	–	n. d.	–	+	–	n. d.	–	–	n.d.	–
von Kossa	Calcium	+	+-	–	–	n. d.	n. v.	–	n. d.	–	+	–	n. d.	–	–	n.d.	–
Alizarin Red S	Calcium	–	–	–	–	n. d.	n. v.	–	n. d.	–	+-	–	n. d.	–	–	n.d.	–
Arnow Staining	L-DOPA	–	–	–	–	n. d.	n. v.	–	n. d.	–	–	–	n. d.	–	–	n.d.	–
Sudan Black B	Lipids	+	+-	n.s.	n. s.	n. d.	n. v.	n.s.	n. d.	n.s.	+-	n.s.	n. d.	n. s.	n.s.	n.d.	n.s.

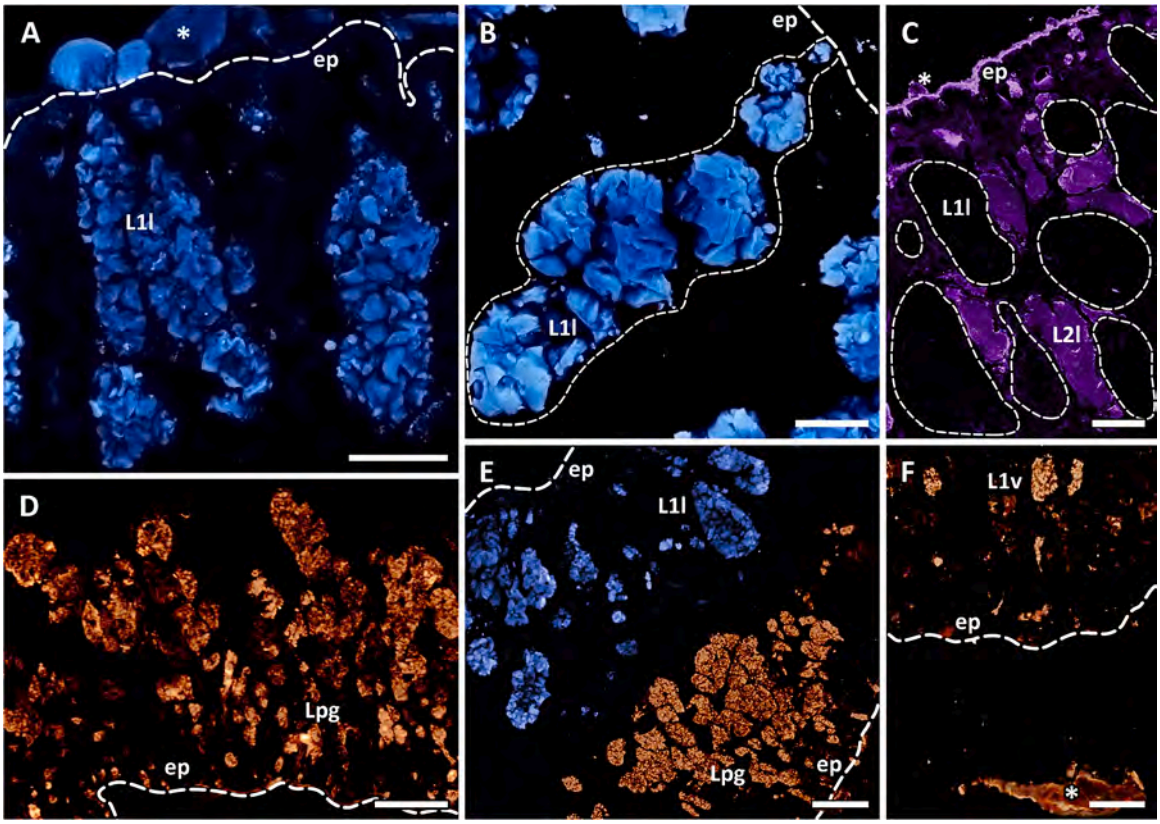

Fig. 6. Lectin affinity tests of the pedal gland cell types in *Latia neritoides*. (A, B) The granular content as well as secreted mucus (white asterisk in A) of L1l (blue) show a positive reaction to the tested lectin *Vicia villosa* Lectin (VVL) and biotinylated *Griffonia* (Bandeiraea) *simplicifolia* Lectin I (GSL1), while the secretory content of L2l (violet) reacts to wheat germ agglutinin (WGA) (C). (D) The gland cell type Lpg (orange) reacts positive for *Ulex europaeus* agglutinin (UEA1). (E) L1l and the glandular content of Lpg (orange) reacts to *Vicia villosa* Lectin (VVL). (F) A positive reaction to the lectin biotinylated *Griffonia* (Bandeiraea) *simplicifolia* Lectin I (GSL1) is visible for the gland cell type L1v (orange). For all panels, the thick dotted line marks the epithelium, the thinner line the gland borders. The asterisks are marking the mucus. Scale bar in images A, B, C and F 25 μm, in image D and E 50 μm.

The third and least abundant gland cell type is N3l with a knobbly shape and very densely packed vesicles (Fig. 10B, C). The vesicles measured 0.6–1.2 μm in diameter and display dotted and striated electron dense and lucent patterns (Fig. 10C). Discharged content was not observed. The abovementioned storage (Ns) is present in the same area, crammed with roundish packets of 0.8–1.5 μm (Fig. 10E), whose role was not identifiable.

The pedal gland cells (Npg) are stuffed with filamentous patterned vesicles (size 0.9–1.6 μm) which are released through bundles of ducts into a ventral groove.

The most common gland cell type ventrally is N1v, with vesicles measuring 0.7–1 μm in diameter and a dotted pattern (Fig. 10F, G). Discharged vesicles close to the duct openings dissolve with increasing distance (Fig. 10F). In contrast, the uniformly electron-dense vesicles of N2v merge before release (Fig. 10H). Their size ranges from 1 to 1.8 μm.

3.2.2. *Histochemistry and lectin affinity of the lateral and ventral glands*

Due to their small size and uniformly positive reaction to histochemical staining, it was not possible to distinguish the lateral gland cell types in the paraffin sections. At least the most abundant gland cell types, N1l and N2l, contain sulphated and carboxylated glycoproteins indicated by the positive Alcian blue (both pH levels) and PAS staining (Fig. 11B, Table 1). There are no detailed data for N3l. The positive lectin affinity test for PNA indicates the presence of galactose linked to N-acetyl galactosamine as a sugar component (supplemental fig. 3; Table 2). All other applied stainings are negative. The storage structure (Ns) does not show any positive reaction at all (Fig. 11C, Table 1).

Similarly, it was also not possible to distinguish the ventral gland cell types. The reported reactivity applies to the most abundant type N1v. No differentiated statement is possible for N2v. Gland cell contents stain weakly for sulphated and carboxylated glycoproteins (positive Alcian blue and PAS staining; Fig. 11D, F, Table 1). The lectin affinity tests reveal the presence of galactose linked to N-acetyl galactosamine (PNA), but also mannose-linked sugar moieties are detected (GNL) (supplemental figs. 3 A, C, Table 2). The positive toluidine blue – O staining indicates the presence of acidic proteins, too (Fig. 11A, Table 1).

The pedal foot gland Nfg in *Neritina* sp. differs from the N1v only in the intensity of the histochemical staining (Table 1). Here, the Alcian blue staining (both pH levels) is more intense than for L1v, whereas the toluidine blue – O staining shows only a weak reaction (Fig. 11A, D, F, Table 1). Galactose linked to N-acetyl galactosamine (PNA) is a sugar component of this pedal gland, too (supplemental fig. 3A, Table 2).

3.2.3. *Histochemistry and lectin affinity of the mucus*

The trail mucus of *Neritina* sp. reacts positively for sulphated & carboxylated glycoproteins (positive AB at pH levels 1.0, 2.5 - Fig. 11E- and PAS staining) as well as acidic (Tol-O pH level 4.5) and basic proteins (BS at all pH levels) (Table 1). In the mucus the sugar galactose linked to N-acetylgalactosamine (PNA) and N-acetylgalactosamine (WGA), while mannose-associated moieties (GNL) could be identified through lectin affinity tests (Table 2). Calcium (positive Alizarin red S and von Kossa staining) and lipids (positive Sudan black B staining) were also detected in the trail mucus (Table 1).

3.2.4. *Element analysis of tissue and mucus*

In contrast to both mucus types of *L. neritoides,* the trail mucus of *Neritina* sp. contained high amounts of calcium (2.98 at%) and phosphorus (2.26 at%). Magnesium (0.27 at%) and sulphur (0.14 at%) were

Table 2
Summary of the lectin affinity tests on mucus and tissue of *Latia neritoides* and *Neritina* sp. Lectin types, the lectin acronym and lectin specificity are listed. Tests with the lectins UEAII, SJA, MAL, LCA, PHAE-E, PHA-L, PSA, DSL, ECL, EEL, DBA do not show a reaction and therefore are not listed. ++ = strong positive reaction; + = positive reaction; +- = weak reaction; - = no reaction; n.d. = not differentiable, n.t. = not tested.

Abbreviation	Lectin type	Specificity	*Latia neritoides* defence mucus	*Latia neritoides* trail mucus	*Latia neritoides* pedal gland system	*Neritina* sp. trail mucus	*Neritina* sp. pedal gland system
ConA	Concanavalin agglutinin	α-linked mannose	+	++	+- L1v, + Lpg	–	n.t.
VVL	*Vicia villosa* Lectin	N-Acetylgalactosamine type (GalNAca (1,3)Gal)> blood group A	+	+	+ L1l, +- L2l, ++ L1v, + Lpg	–	n.t.
WGAs	Succinylated Wheat germ agglutinin	N-acetylglucosamine, no sialic acid residues	+	+	+- in L2l, ++ L1v	–	n.t.
GSL I	Biotinylated *Griffonia* (Bandeiraea) *simplicifolia* Lectin I	N-Acetylgalactosamine (GalNAc) > Gal	+	–	+- L1l, + L1v, + Lpg	–	n.t.
PNA	Peanut agglutinin	Galactose linked to N-acetylgalactosamine (Galβ(1,3) GalNAc)>GalNH$_2$ >Lac	+	–	+- L1v	+	++ N1l/N2l (N3l n.d.), ++ N1v (N2v n.d.), ++ Npg
SNA I	*Sambucus nigra* agglutinin	Sialic acid linked to N-acetylgalactosamine or galactose	+	–	–	–	n.t.
WGA	Wheat germ agglutinin	N-Acetylglucosamine (oligomer>monomer>NANA)	+-	++	+- in L2l, + L1v	+	–
GSL II	Biotinylated *Griffonia* (Bandeiraea) *simplicifolia* Lectin	N-Acetylgalactosamine (oligomer>monomer)	–	+	+ Lpg	–	n.t.
UEA I	*Ulex europaeus* agglutinin	α-linked fucose > Fuca(1–2)Galβ(1–3) GalNA	–	+	+ L1l, + Lpg	–	n.t.
STL	*Datura stramonium* lectin	N-Acetyl-D-glucosamin type (GlcNAcβ (1,4))	–	+	–	–	n.t.
GNL	Galanthus nivalis agglutinin	Mannose linked (Mana(1,3)Man)	–	–	+ L2l, +- L1v	+	+- N1v (N2v n.d.)
JACALIN	*Artocarpus integrifolia* lectin	Galactose linked to N-acetylgalactosamine (Galβ(1,3)GalNAc)	–	–	+ L2l, +- L1v	–	n.t.
SBA	Soybean agglutinins	N-Acetylgalactosamine (GalNAc) > Gal	–	–	+- L1v	–	n.t.
LEL	*Lycopersicon esculentum* lectin	N-acetylglucosamine, (GlcNAcβ1–4)1–4	–	–	+- L1v	–	n.t.

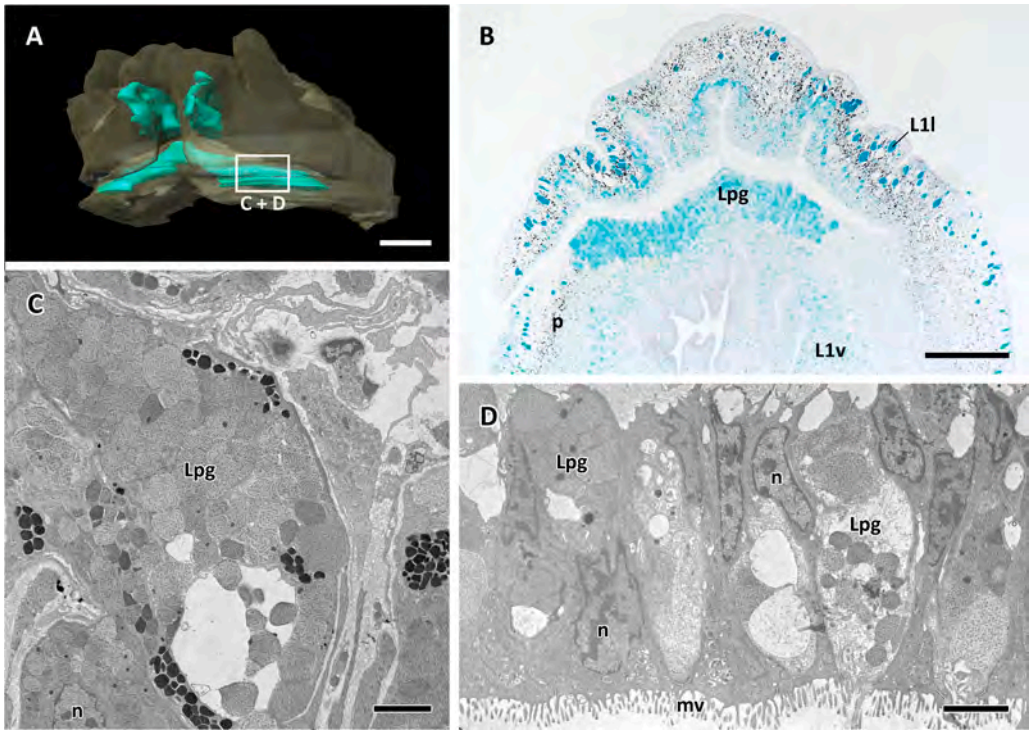

Fig. 7. *Latia neritoides,* presentation of the gland area Lpg (*Latia* pedal gland), based on histochemical and ultrastructural determinations. (A) Overview of the area where Lpg (turquoise) is situated. (B) Sulphated mucosubstances are present in L1l, L1v and Lpg as indicated by the strong positive reaction of the Alcian blue staining (pH 1.0). The distribution of pigmentation in the investigated area (p) is visible. (C, D) The transmission electron images show a similar appearance of the granulated material of Lpg as in L1v with an electron dense/lucent pattern inside the vesicles. Additionally labelled: mv = microvilli, n = nucleus. Scale bars in image A and B 500 μm and in image C and D 2.5 μm.

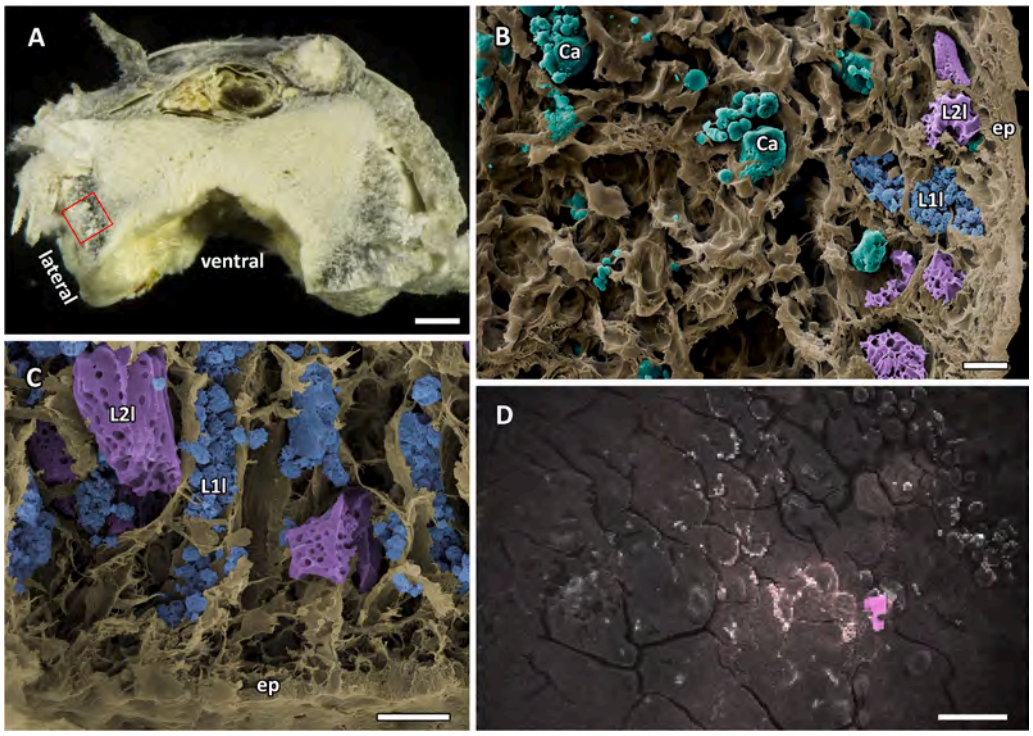

Fig. 8. *Latia neritoides,* scanning electron images of the pedal gland area and defence mucus. (A) Overview of a cross section of *L. nerotides*, where the investigated area is marked with a red square. (B and C) Laterally the calcium deposits (Ca = turquoise) and gland types L1l (blue) and L2l (violet) can clearly be recognised beneath the foot epithelium (ep). (D) The dot-mapping of the defence mucus reveals silicon containing areas in dark pink and chlorine in light pink. Additionally labelled: ep = epithelium. Scale bars in image A 400 μm, in image B and C 20 μm and in image D 100 μm.

Table 3
Proportion of elements in atom percent (at%) in mucus, gland cells, and tissue of *Latia neritoides* and *Neritina* sp., resulting from EDAX element analyses.

	Ca	Na	Mg	P	S	Cl	K	Fe	Si	F
***L. neritoides* trail mucus**										
***L. neritoides* defence mucus sampling in 2019**	0.19	1.13	0.21	0.16	0.41	0.75	0.15	–	–	–
***L. neritoides* defence mucus sampling in 2020**	0.14	0.99	0.14	0.32	0.39	0.79	0.19	–	–	–
***L. neritoides* L1l**	0.29	0.22	0.45	0.62	0.28	–	0.18	–	–	–
***L. neritoides* L2l**	0.32	0.14	0.2	0.12	0.46	0.14	–	–	–	–
***L. neritoides* Ca**	5.65	0.12	1.85	0.22	0.19	–	–	–	–	0.19
***Neritina* sp. trail mucus**	2.98	–	0.27	2.26	0.14	–	–	–	–	–
***Neritina* sp. granulae N1l/N2l/N3l**	0.59	0.46	–	0.36	0.99	0.43	0.24	0.12	–	–
***Neritina* sp. N1v/N2v**	–	0.46	–	0.50	0.52	0.27	0.20	–	–	–
***Neritina* sp. granulae N1v/N2v**	–	0.21	–	0.35	0.87	0.16	0.21	–	–	–
***Neritina* sp. granulae Nc/N1v/N2v**	–	0.24	–	0.45	0.49	0.2	0.24	–	–	–
***L. neritoides* river water**	0.33	1.01	0.33	–	0.19	–	–	0.61	2.84	–
***Neritina* sp. aquarium water**	1.88	–	0.63	–	0.14	–	–	0.19	0.22	–
Alu stub	–	–	0.16	–	–	–	–	0.26	0.22	–

present at much lower concentrations. Calcium, magnesium and sulphur were also detected in the aquarium water and could have affected the results (Table 3). Phosphorus and sulphur concentrations were relatively high in all analysed lateral and ventral granules (P: 0.35–0.50 at%; S: 0.49–0.99 at%). A detailed assignment to the gland cell types was not possible in this case. Again, copper was disregarded because of the high concentration in the stub and in the aquarium water (1.08 at%).

4. Discussion

Our aim was to characterize the gland cells in the lateral and ventral foot areas of both *L. neritoides* and *Neritina* sp. to infer potential sources of the glowing 'defence' mucus of *L. neritoides*. We found no direct evidence of the pedal mucus secretions contributing to the defence mucus. However, the morphological and histochemical differences between gland areas and species demonstrated here indicate a possible role of the gland cells in the lateral foot area in defence mucus production. The only large and multicellular gland in the anterior region of the foot in *L. neritoides* and *Neritina* sp. is the typical pedal gland that is generally considered the main source of trail mucus for gastropods (Smith and Stanisic, 1998). The glands position and similarity in cell morphology make this gland an unlikely contributor to the defence mucus in *L. neritoides*, calling for a careful analysis of indications for this role in the lateral pedal gland cells. Based on the reports by Bowden (1950), we have expanded the available information on this species.

4.1. Comparison of the Latia neritoides and Neritina sp. foot gland system

The main difference between the two species concerns the lateral gland area of the foot. In *L. neritoides* the gland cells are all subepithelial, while in *Neritina* sp. they are epithelial. Based on the position of the glands it is possible that the epithelial gland cells in *Neritina* sp. (N1l, N2l, N3l) are mucocytes (Grenon and Walker, 1978) and are responsible for the reduction of friction and are used in lubrication. The differentiation of these gland cell types is based on the appearance of granules in TEM pictures, but not on granule shape or size. In *L. neritoides* such a gland type was not apparent in the lateral epithelium.

In *L. neritoides* two large gland types (L1l, L2l), absent in *Neritina* sp., were densely distributed over the entire lateral foot area. They were termed "mucous" and "granular" cells by Bowden (1950) and

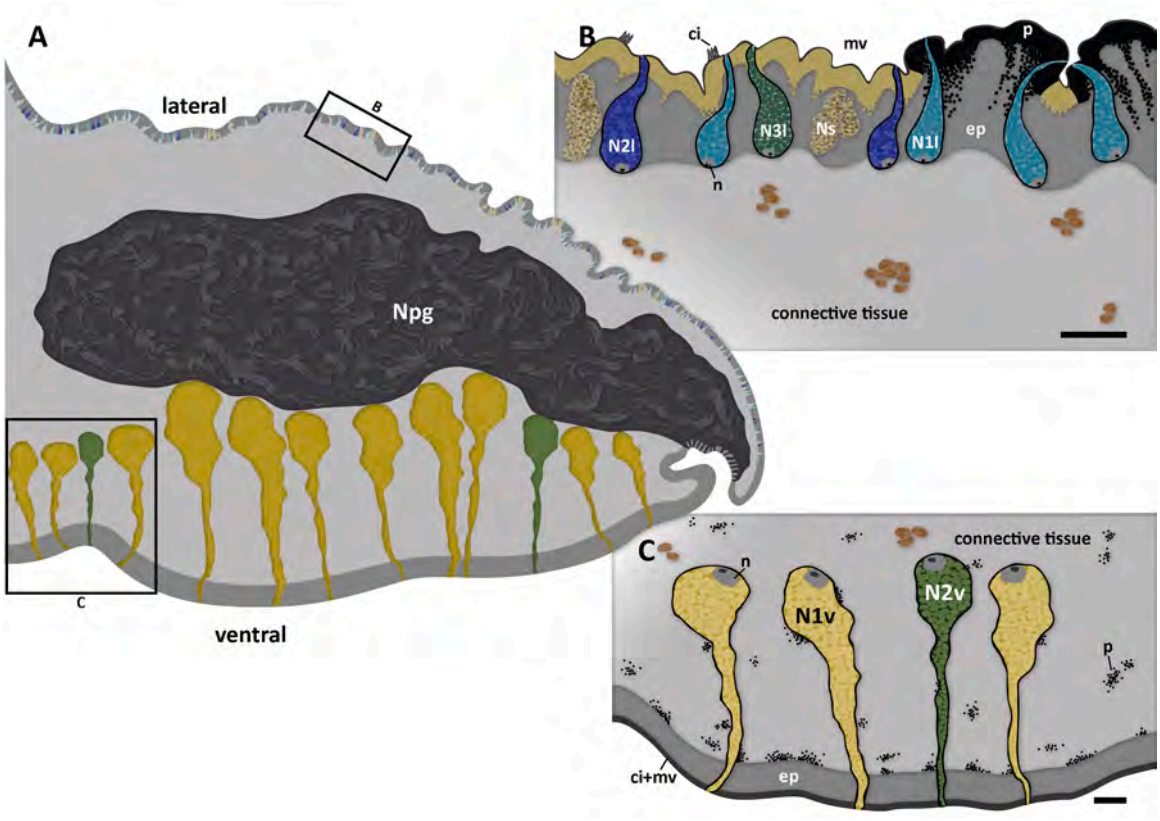

Fig. 9. *Neritina* sp., schematic overview and detailed visualisation of the pedal gland system in the foot. (A) Distribution pattern of the gland cell types present. In contrast to the lateral glands cells the ventral glands are situated subepithelially. A voluminous pedal gland (Npg, *Neritina* pedal gland, = dark grey) is visible in the anterior part of the foot. (B) Detailed visualisation of the epithelial glands cell types (N1l = light blue, N2l = dark blue, N3l = green) of the lateral area. Between the glands a storage structure (Ns = yellow dotted) with unknown material is visible. A strong pigmentation (p), varying between black and brown, is obvious in the epithelial layer (ep). (C) Two gland cell types (N1v = yellow, N2v = light green) are present in the ventral area. Here the black pigmentation is spread throughout the whole gland area, but is less strong than in the lateral area. Cilia (ci) and microvilli (mv) are present in high numbers in contrast to the lateral area, where cilia are only sporadically present. Additionally labelled: n = nucleus. Scale bar in image B 20 μm, in image C 50 μm.

considered to be responsible for the luminous mucus. There are several aspects that suggest that those glands play a role also in the defence secretion: i) In stress situations a large volume of mucus is secreted within a very short time (Meyer-Rochow and Moore, 1988; Greistorfer, pers. observation). The large sizes and high numbers of L1 and L2l cells in the lateral pedal area where the defence mucus is discharged make these gland cells plausible candidates for the source of the mucus; ii) The results of the histochemical staining of L1l correspond to the defence mucus (sulphated, carboxylated glycoproteins present); and iii) The lectin affinity tests show similarities between the glands and the defence mucus (sulphated, carboxylated glycoproteins present). However, the glowing component is released only in the pneumostome area at the right posterior side of *L. neritoides* (Meyer-Rochow and Moore, 1988; Greistorfer, pers. observations). Thus, although L1l and L2l may be involved in the defence secretion, at least one component responsible for the glow seems to be produced by other gland cell types in a different place.

In *L. neritoides* as well as in *Neritina* sp. a pedal gland (Lpg; Npg) occupies the anterior part of the foot. This gland differs in the way the mucus is released. In *Neritina* sp. the gland cells discharge their secretions through a few ducts opening in a groove in the ventral side of the foot. In *L. neritoides,* however, these specific gland cells discharge through individual ducts over a large part of the anterior foot area.

Another remarkable difference between the species is the presence of calcium deposits in the foot of *L. neritoides*. It is not clear whether this calcium deposits are used for shell biomineralization or released with the mucus since no connection to any gland structure is detectable. Such deposits are missing in *Neritina* sp. Calcium is known for its potential role in adhesives (Smith, 2002) and may therefore, in combination with the peculiar gland cell types in the lateral foot area of *L. neritoides*, be linked to the defence mucus production.

Besides these differences, there are obvious similarities between *L. neritoides* and *Neritina* sp. The ventral pedal epithelia are similar with regard to the number, distribution, and shape of the gland cells. Also, in both species the ventral epithelium is thicker and more densely ciliated than the lateral epithelium, which may reflect the common function of producing trail mucus.

4.2. Comparison of mucus types of Latia neritoides and Neritina sp

Based on a comparison of the histochemical staining results, no species differences were detected between mucus types, *i.e. L. neritoides* trail and defence mucus and *Neritina* sp. trail mucus. This may be related to the fact that the stains provide only a broad overview on the mucus chemical components. More specific lectin affinity tests, however, revealed some differences. We found branched N-linked hexasaccharides, N-galactosamine (GalNAc) and N-acetylglucosamine (GlcNAc) were detected (positive reactions to Con A, VVL, WGAs) in both mucus types produced by *L. neritoides,* but not in the trail mucus of *Neritina* sp. In contrast, only the trail mucus of *Neritina* sp. reacts positive for α-linked mannose. Complex glycosylation with galactose (galactose linked to GalNAc) was present both in the trail mucus of *Neritina* sp. and the defence mucus of *L. neritoides.* Generally, it is not straightforward to link a gland cell type to one of the mucus types based on lectin affinity tests. However, for GSL2 and STL (both specific for different GlcNAc structures) as well as for UEA1 (specific for α-fucose) only the trail

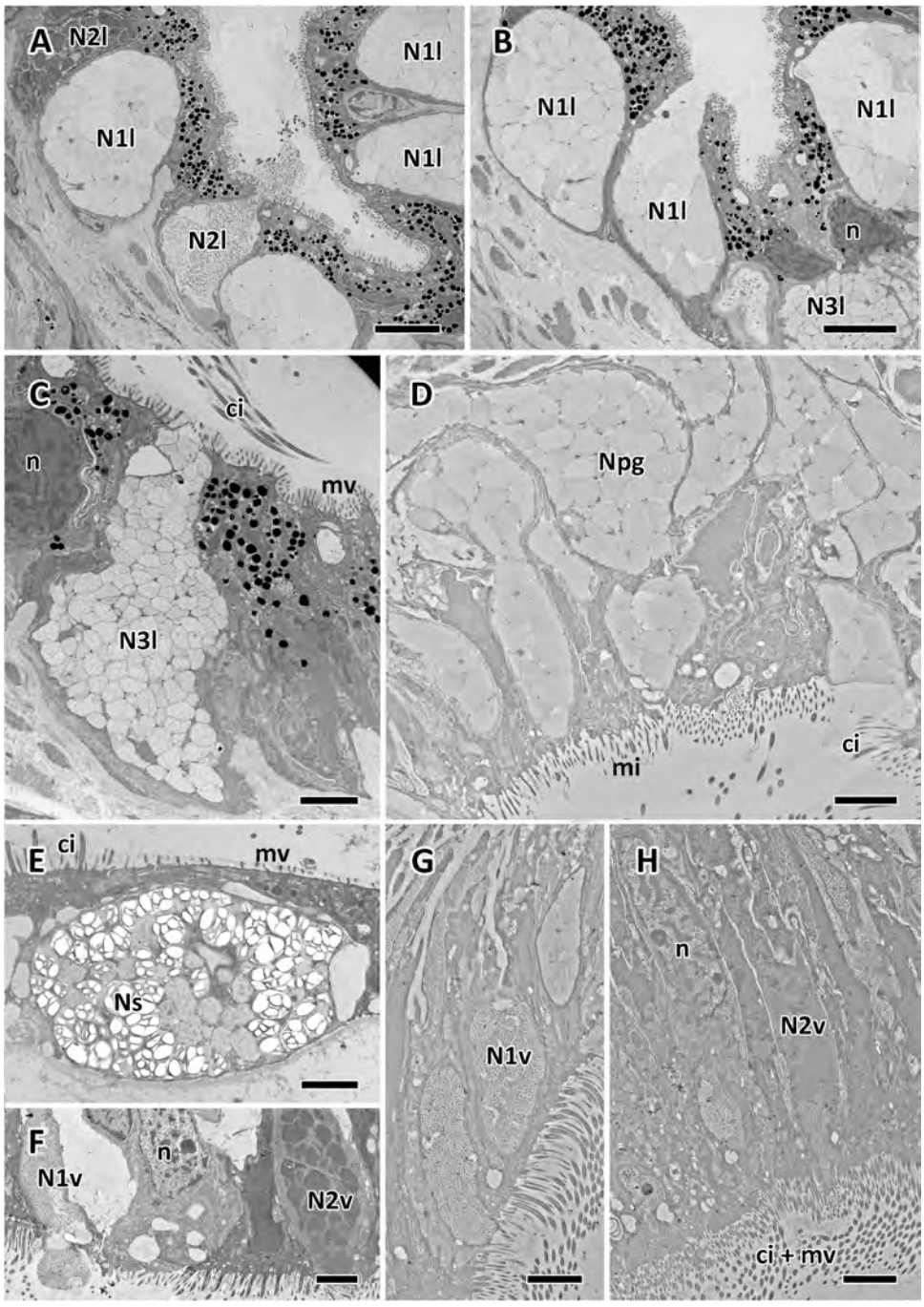

Fig. 10. *Neritina* sp., transmission electron micrographs (TEM) of the pedal gland area. (A, B) In the lateral epithelium the gland cell types N1l and N2l are positioned next to each other with a different electron dense appearance of the vesicles. The release of the mucus is visible. (C) The vesicles of N3l display a dotted pattern in the TEM sections. (D) The ducts of the pedal gland (Npg = *Neritina* pedal gland) contain filamentous patterned vesicles. (E) In the lateral area a storage structure (Ns), filled with spheroidal packages, is apparent. (F) A comparison of the granulated material of N1v and N2v. (G) N1v produces electron transparent vesicles with a dotted pattern. (H) The vesicles of N2v are of a uniform appearance, but disassemble prior to being ejected. Differences in the distributions of the cilia (ci) and the microvilli (mv) become apparent in the lateral (C, E) and ventral (H) gland areas and the ventrally opening groove (D). Additionally labelled: n = nucleus. Scale bars in images A and B 5 μm and in images C, D, E, F, G and H 2.5 μm.

mucus of *L. neritoides* gave a positive reaction. UEA1 gave a positive reaction in lateral and ventral gland types, but for GSL2 positive staining was detected only in Lpg. This leads to the conclusion that this latter gland type has presumably functions in the release of the trail mucus of *L. neritoides*.

When there was a positive reaction of the defence mucus, there was also a positive reaction in one or more gland types of *L. neritoides.* Only the lectin SNA1 was not detectable in any of the pedal gland cells, suggesting this substance is secreted in a different location.

It was surprising that the trail mucus did not show any reaction in the lectin affinity tests for GSL1 and PNA. This was in contrast to the ventrally located gland types and may be due to differences in the sampling process of mucus and tissue. VVL, WGA, WGAs, GSL1 gave positive reactions in connection with one or both common lateral gland types (L1l/L2l) and the defence mucus, but this has to be seen as only a weak indicator for a correlation between them.

4.3. Comparison of Latia neritoides with other aquatic gastropods

Gastropods living in periodically or constant fast-flowing water bodies such as rivers or wave-exposed shores need to adhere firmly to the substrate to avoid detachment by water currents. Although little is known on mucus-aided adhesion in freshwater species, marine limpets such as *Patella* sp. (Patellogastropoda) are well investigated in this respect. Six out of nine pedal gland cell types of *P. vulgata* discharge through the ventral epithelium (Grenon and Walker, 1978), compared to only two in *L. neritoides*. This may indicate that limpets attach themselves to the substrate by means of an adhesive mucus (Smith, 2002)

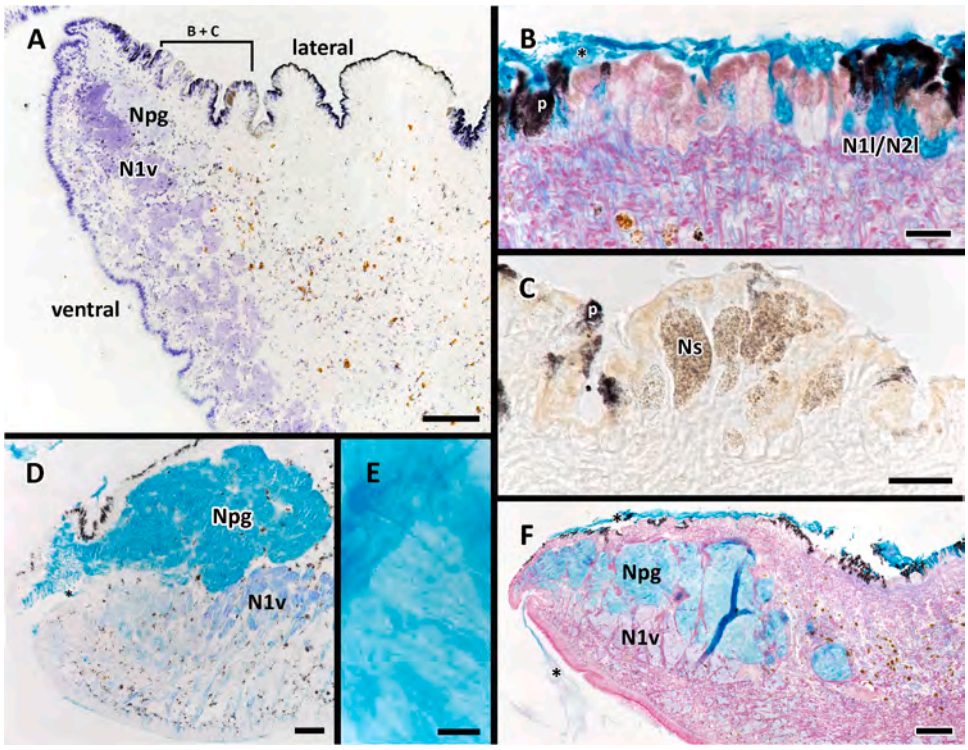

Fig. 11. *Neritina* sp., histochemical analyses of the gland system in the foot and the released mucus. (A) Overview of a part of the foot with different gland cell types (N1v, Npg = *Neritina* pedal gland) reacting positive to Toluidine blue - O (pH 4.5). (B) Positive reaction in the gland cell type N1l/N2l to Alcian blue (pH 1.0; in combination with Azan) is evident. (C) No reaction of the storage structure (Ns) in Biebrich scarlet at pH 9.5 is detectable. (D) The pedal gland (Npg) and the ventral gland cell type N1v give a positive reaction to the combination stain of Alcian blue – periodic acid-Schiff (AB-PAS) at pH 1.0. (E) Positive mucus reaction to Alcian blue (AB) at pH 2.5. (F) Npg and N1v stain positive with Alcian blue (pH level 1.0) and Azan in combination. (B, D, F) Positive reaction to AB pH level 1.0 of the released mucus (asterisks). (C, F) Strong pigmentation (p) of the lateral foot epithelium is apparent. Scale bars in image A and F = 100 μm, in image B and C = 20 μm and in image D and E = 50 μm.

requiring additional gland cell types. In regard to the histochemical staining results as well as the morphological appearance and location of the gland cell types in the investigated limpet *P. vulgata* (P1 – P9), L1l and L2l cannot be directly compared to any of the identified gland types, because different histochemical stains were used. Nevertheless, the gland cell types P2 and P5 are the ones most similar to L1v and L2v in regard to the location, but secrete an adhesive mucus in contrast to L1v and L2v (Grenon and Walker, 1978).

A comparison of the substances present in the gland cells in *L. neritoides* with those of abalone species shows that the subepithelial gland types of both taxa contain sulphated & carboxylated glycoproteins (Lee et al., 1999). However, no glands similar to *L.* neritoides L1l or L2l are mentioned for the abalone species.

Compared to the four described pedal gland cell types (M1 – M4) in *Crepidula dilatata,* a slipper snail, only one is subepithelial and comparable to the L1v and L2v. The type M4 of *C. dilatata* with its elongated shape and long duct resembles Lv1 and Lv2, but contains more homogenous material than is present in *L. neritoides* (Chaparro et al., 1998) and is thought to be involved in adhesion to older individuals.

In *Trimusculus costatus* (Trimusculidae), a species that uses a specific mucus for defence (Pinchuck and Hodgson, 2011), three different gland cell types that are considered to be responsible for the defence mucus production have been described. These defence mucous gland cells show some similarities to L1l and L2l of *L. neritoides* in that they all are large subepidermal cells with separate ducts and there are similarities in the reaction of the gland content to histochemical staining (Pinchuck and Hodgson, 2011).

Lectin affinity tests are not published for the above mentioned aquatic gastropods species.

5. Conclusion and outlook

We found that *L. neritoides* differs in two gland cell types in the lateral pedal epithelium from *Neritina* sp., and from several other marine gastropods where published data are available. These differences lead to the conclusion that the gland types L1l and L2l may be involved in the mucus defence system of *L. neritoides*. The locally restricted release of the glowing defence mucus, however, indicates that one or more important mucus components (such as the purple protein) are produced somewhere in, or close to the opening of, the mantel cavity.

Future studies focusing on the pneumostome area and the deeper parts of the mantle cavity using modern technologies like μ-CT and HREM combined with ultrastructural analyses will likely yield further insights into the gland system of the defensive mechanism of *L. neritoides*. In addition, research employing gel electrophoresis combined with MS and transcriptome analyses is already ongoing research in our lab and will help to explore the protein composition of the different mucus types in *L. neritoides.*

Ethics approval and consent to participate

This study followed the guidelines from the Directive 2010/63/EU.

Consent for publication

Not applicable.

Funding

Sophie Greistorfer was recipient of a DOC Fellowship of the Austrian Academy of Sciences (DOC [Doctoral Fellowship Programme of the Austrian Academy of Sciences] / 25023). COST (European Cooperation in Science and Technology) financed the STSM grant (ECOST-STSM-CA15216-080419-106146) for lectin affinity tests. Robert Farkas was funded by VEGA 2/0103/17 and APVV-16-0219.

CRediT authorship contribution statement

JvB, GS and SG conceived and designed the study. JvB and GS supervised the study. JvB, SG and VBM-R collected field data. SG collected, analyzed and interpreted the data. The stay in Bratislava was under supervision of RF. SG wrote the first draft, GS, IM, JvB, VBM-R and RF revised the manuscript. All authors read and approved of the final manuscript at submission.

Declaration of Competing Interest

The authors declare that they have no known competing financial interests or personal relationships that could have appeared to influence the work reported in this paper.

Data Availability

Data will be made available on request.

Acknowledgments

We like to thank the Department of Evolutionary Biology, Unit Integrative Zoology, University of Vienna Austria, for hosting the study. We particularly thank Mag. Christian Baranyi for an introduction to the DNA lab and help with the protocol setup for the DNA extraction, Nikolaus Helmer, BSc for the help with analysing the CO1 sequences and Julian Bibermair, MSc for help with the handling of the 3D data. Further we thank Johannes Suppan, MSc for providing most of the TEM sections, Kevin Pfeifer, MSc (Archaea Biology and Ecogenomics Unit) and Margret Eckhardt, MSc for the possibility to contrast them with uranyl acetate. We also like to thank Mag. Daniela Gruber from the Core Facility Cell Imaging and Ultrastructure Research (University of Vienna Austria) for her advisory activity at the SEM. Also thanks to the participants of the class "Spezielle Techniken in der Elektronenmikroskopie und Ultrastrukturforschung (2021)", in particular Tabita Bächle. Furthermore, we wanted to thank Brian Smith (Freshwater Ecologist, NIWA, Hamilton, New Zealand) for the outstanding cooperation and the provision of a work place.

Appendix A. Supporting information

Supplementary data associated with this article can be found in the online version at doi:10.1016/j.zool.2022.126067.

References

Abdou, A., Galzin, R., Lord, C., Denys, G.P.J., Keith, P., 2017. Revision of the species complex "Neritina pulligera" (Gastropoda, Cycloneritimorpha: Neritidae) using taxonomy and barcoding. Vie Milieu - life evironment 67, 149–161.

Aescht, E., Büchl-Zimmermann, S., Burmester, A., Stefan, D.-P., Desel, C., Hamers, C., Jach, G., Kässens, M., Makovitzky, J., Mulisch, M., Nixdorf-Bergweiler, B., Pütz, D., Riedelsheimer, B., van den Boom, F., Wegerhoff, R., Welsch, U., 2010. Romeis Mikroskopische Technik, 18th ed. Spektrum Akademischer Verlag, Heidelberg.

Anctil, M., 2018. Luminous Creatures: The History and Science of Light Production in Living Organisms. McGill-Queen's University Press, Montral & Kingston, London, Chicago. ⟨https://doi.org/10.2307/J.CTV1FXN06⟩.

Baker, H.B., 1923. Notes on the radula of the Neritidae. Proc. Acad. Nat. Sci. Phila. 75, 117–178.

Barrientos, Z., 2020. A new aestivation strategy for land molluscs: hanging upside down like bats. UNED Res. J. 12, e2802 https://doi.org/10.22458/urj.v12i1.2802.

Bingham, F.O., 1972. The mucus holdfast of *Littorina irrorata* and its relationship to relative humidity and salinity. Veliger 15, 48–50.

Böhm, A., Oppel, A., 1919. Taschenbuch der mikroskopischen Technik - Anleitung zur mikroskopischen Untersuchung der Gewebe und Organ der Wirbeltiere und des Menschen unter Berücksichtigung der embryologischen Technik, 8th ed. R. Oldenbourg, München.

Bouchet, P., Rocroi, J.P., Hausdorf, B., Kaim, A., Kano, Y., Nützel, A., Parkhaev, P., Schrödl, M., Strong, E.E., 2017. Revised classification, nomenclator and typification of gastropod and monoplacophoran families. Malacologia 61, 1–526. https://doi.org/10.4002/040.061.0201.

Bowden, B.J., 1950. Some observations on a luminescent freshwater limpet from New Zealand. Biol. Bull. 99, 373–380. https://doi.org/10.2307/1538467.

von Byern, J., Cyran, N., Klepal, W., Rudoll, L., Suppan, J., Greistorfer, S., 2018. The structure of the cutaneous pedal glands in the banded snail *Cepaea hortensis* (Müller, 1774). J. Morphol. 279, 187–198. https://doi.org/10.1002/jmor.20763.

von Byern, J., Farkaš, R., Steinort, D., Greistorfer, S., Eckhard, M., Cyran, N., 2021. Perspective for a New Bioinspired Permanent Adhesive for dry Conditions - Insights in the Glue Producing Japanese art of Defence System of the Oita Salamander *Hynobius dunni*. Front. Mech. Eng. 7, 1–14. https://doi.org/10.3389/fmech.2021.667857.

Chaparro, O.R., Bahamondes-Rojas, I., Vergara, A.M., Rivera, A.A., 1998. Histological characteristics of the foot and locomotory activity of *Crepidula dilatata* Lamarck (Gastropoda: Calyptraeidae) in relation to sex changes. J. Exp. Mar. Biol. Ecol. 223, 77–91. https://doi.org/10.1016/S0022-0981(97)00151-2.

Chapman, M.G., Underwood, A.J., 1996. Influences of tidal conditions, temperature and desiccation on patterns of aggregation of the high-shore periwinkle, *Littorina unifasciata*, in New South Wales, Australia. J. Exp. Mar. Biol. Ecol. 196, 213–237. https://doi.org/10.1016/0022-0981(95)00131-X.

Counsilman, J.J., Ong, P.P., 1988. Responses of the luminescent land snail *Dyakia (Quantula) striata* to natural and artificial lights. J. Ethol. 6, 1–8. https://doi.org/10.1007/BF02348856.

Counsilman, J.J., Loh, D., Chan, S.Y., Tan, W.H., Copeland, J., 1987. Factors affecting the rate of flashing and loss of luminescence in a Asian land snail, *Dyakia striata*. Veliger 29, 394–399.

Deheyn, D.D., Wilson, N.G., 2011. Bioluminescent signals spatially amplified by wavelength-specific diffusion through the shell of a marine snail. Proc. R. Soc. B Biol. Sci. 278, 2112–2121. https://doi.org/10.1098/rspb.2010.2203.

Denny, M., 1983. Molecular Biomechanics of Molluscan Mucous Secretions, Metabolic Biochemistry and Molecular Biomechanics. ACADEMIC PRESS, INC., Seattle Washington. ⟨https://doi.org/10.1016/b978-0-12-751401-7.50017-x⟩.

Greistorfer, S., Klepal, W., Cyran, N., Gugumuck, A., Rudoll, L., Suppan, J., von Byern, J., 2017. Snail mucus – glandular origin and composition in *Helix pomatia*. Zoology 122, 126–138. https://doi.org/10.1016/j.zool.2017.05.001.

Greistorfer, S., Suppan, J., Cyran, N., Klepal, W., Farkas, R., Rudoll, L., von Byern, J., 2020. Characterization of the *Arion vulgaris* pedal gland system. J. Morphol. 281, 1059–1071. https://doi.org/10.1002/jmor.21231.

Grenon, J.F., Walker, G., 1978. The histology and histochemistry of the pedal glandular system of two limpets, *Patella vulgata* and *acmaea tessulata* (gastropoda: Prosobranchia). J. Mar. Biol. Assoc. U. Kingd. 58, 803–816. https://doi.org/10.1017/S0025315400056770.

Haneda, Y., 1985. Luminous organisms. Kouseisha-kouseikaku, Tokyo.

Harvey, E.N., 1952. Bioluminescence. Academic Press, New York.

Isobe, M., Uyakul, D., Sigurdsson, J.B., Goto, T., Lam, T.J., 1991. Fluorescent substance in the luminous land snail, *Dyakia striata*. Agric. Biol. Chem. 55, 1947–1951. https://doi.org/10.1080/00021369.1991.10870892.

Kiernan, J.A., 1999. Histological and Histochemical Methods: Theory and Practice, 3rd ed. Butterworth-Heinemann, Oxford.

Kumar, S., Stecher, G., Li, M., Knyaz, C., Tamura, K., 2018. MEGA X: Molecular evolutionary genetics analysis across computing platforms. Mol. Biol. Evol. 35, 1547–1549. https://doi.org/10.1093/molbev/msy096.

Lee, C., Moon, D.Y., Jee, Y.J., Choi, B.T., 1999. Histochemistry of mucosubstances on the pedal sole of five abalone species. Korean J. Biol. Sci. 3, 253–258. https://doi.org/10.1080/12265071.1999.9647494.

Marshall, B.A., 1997. A luminescent eulimid (Mollusca: Gastropoda) from New Zealand. Mollusca Res 18, 69–72. https://doi.org/10.1080/13235818.1997.10673683.

Meyer-Rochow, V.B., Moore, S., 1988. Biology of *Latia neritoides* GRAY 1850 (Gastropoda, Pulmonata, Basomatophora): the only light-producing freshwater snail in the world. In: Int. Rev. der gesamten Hydrobiol. und Hydrogr, 73, pp. 21–42.

Meyer-Rochow, V.B., Moore, S., 2009. Hitherto unreported aspects of the ecology and anatomy of a unique gastropod: the bioluminescent freshwater pulmonate *Latia neritoides*. In: Meyer-Rochow, V.B. (Ed.), Bioluminescence in Focus - a Collection of Illuminating Essays. Trivandrum: Research Signpost, Kerala, pp. 85–104.

Morris, N., Taylor, J., 2000. Global events and biotic interaction as controls on the evolution of gastropods. In: Culver, S.J., Rawson, P.F. (Eds.), Biotic Response to Global Change: The Last 145 Million Years. Cambridge University Press, Cambridge, pp. 149–163.

Nicholas, K.B., Nicholas, H.B., 1997. GeneDoc: a tool for editing and annotating multiple sequence alignments. Embnet N. 4, 1–4.

Oba, Y., Schultz, D.T., 2014. Eco-evo bioluminescence on land and in the sea. In: Thouand, G., Marks, R. (Eds.), Bioluminescence Fundamentals and Applications in Biotechnology. Springer-Verlag, Berlin Heidelberg, Heidlberg, New York, Lordrecht, London, pp. 3–36.

Ohmiya, Y., Kojima, S., Nakamura, M., Niwa, H., 2005. Bioluminescence in the limpet-like snail, *Latia neritoides*. Bull. Chem. Soc. Jpn. 78, 1197–1205. https://doi.org/10.1246/bcsj.78.1197.

Ovando, X.M.C., Gregoric, D.E.G., 2012. Systematic revision of *Chilina* Gray (Gastropoda: Pulmonata) from Northwestern Argentina and description of a new species. Malacologia 55, 117–134. https://doi.org/10.4002/040.055.0108.

Pinchuck, S.C., Hodgson, A.N., 2011. Structure of the lateral pedal defensive glands of *Trimusculus costatus* (Gastropoda: Trimusculidae). J. Mollusca Stud. 78, 44–51. https://doi.org/10.1093/mollus/eyr034.

Ponder, W.F., 1988. Bioluminescence in *Hinea braziliana* (Lamarck) (Gastropoda: Planaxidae). J. Mollusca Stud. 54, 361. https://doi.org/10.1093/mollus/54.3.361.

Rambaut, A., 2010. FigTree 3 (1), v1.

Ramesh, C., Meyer-Rochow, V.B., 2021. Bioluminescence in aquatic and terrestrial organisms elicited through various kinds of stimulation. Aquat. Ecol. 55, 737–764. https://doi.org/10.1007/s10452-021-09875-0.

Ronquist, F., Huelsenbeck, J.P., 2003. MrBayes 3: bayesian phylogenetic inference under mixed models. Bioinforma. Appl. NOTE 19, 1572–1574. https://doi.org/10.1093/bioinformatics/btg180.

Shimomura, O., Johnson, F.H., 1968a. Purification and properties of the luciferase and of a protein cofactor in the bioluminescence system of *Latia neritoides*. Biochemistry 7, 2574–2580. https://doi.org/10.1021/bi00847a019.

Shimomura, O., Johnson, F.H., 1968b. The structure of *Latia* luciferin. Biochemistry 7, 1734–1738. https://doi.org/10.1021/bi00845a017.

Shimomura, O., Yampolsky, I., 2019. Bioluminescence - chemical principles and methods, 3rd ed. World Scientific, New Jersey.

Shimomura, O., Johnson, F.H., Kohama, Y., 1972. Reactions involved in bioluminescence systems of limpet (*Latia neritoides*) and Luminous Bacteria. Proc. Natl. Acad. Sci. U. S. A 69, 2086–2089.

Smith, A.M., 1992. Alternation between attachment mechanisms by limpets in the field. J. Exp. Mar. Biol. Ecol. 160, 205–220.
Smith, A.M., 2002. The structure and function of adhesive gels from invertebrates. Integr. Comp. Biol. 42, 1164–1171. https://doi.org/10.1093/icb/42.6.1164.
Smith, A.M., Quick St., T.J., Peter, R.L., 1999. Differences in the composition of adhesive and non-adhesive mucus from the limpet *Lottia limatula*. Biol. Bull. 196, 34–44. https://doi.org/10.2307/1543164.
Smith, B.J., Stanisic, J., 1998. Pulmonata Introduction. Pp.1037-1061. In: Beesley, P.L., Ross, G.J.B., Wells, A. (Eds.), Mollusca: The Southern Synthesis. Fauna of Australia, Vol. 5. CSIRO Publishing, Melbourne.
Verdes, A., Gruber, D.F., 2020. Glowing worms: biological, chemical, and functional diversity of bioluminescent annelids. Integr. Comp. Biol. 57 (1), 18–32. https://doi.org/10.1093/icb/icx017.
Vermej, G.J., 2015. Gastropod skeletal defences: land, freshwater, and sea compared. Vita Malacol. 13, 1–25.
Wilson, T., Hastings, W.J., 2013. Bioluminescence: living lights, lights for living, bioluminescence: living lights, lights for living. Cambridge Mass. Harvard University Press.
Yu, M., Ohmiya, Y., Naumov, P., Liu, Y.-J., 2018. Theoretical insight into the emission properties of the luciferin and oxyluciferin of *Latia*. Photochem. Photobiol. 93, 540–544. https://doi.org/10.1111/php.12876.